

## **Lung Cancer Risk in Mice: Analysis of Fractionation Effects and Neutron RBE with a Biologically Motivated Model**

Author(s): W. F. Heidenreich, B. A. Carnes, H. G. Paretzke

Source: Radiation Research, 166(5):794-801.

Published By: Radiation Research Society

DOI: <http://dx.doi.org/10.1667/RR0481.1>

URL: <http://www.bioone.org/doi/full/10.1667/RR0481.1>

---

BioOne ([www.bioone.org](http://www.bioone.org)) is a nonprofit, online aggregation of core research in the biological, ecological, and environmental sciences. BioOne provides a sustainable online platform for over 170 journals and books published by nonprofit societies, associations, museums, institutions, and presses.

Your use of this PDF, the BioOne Web site, and all posted and associated content indicates your acceptance of BioOne's Terms of Use, available at [www.bioone.org/page/terms\\_of\\_use](http://www.bioone.org/page/terms_of_use).

Usage of BioOne content is strictly limited to personal, educational, and non-commercial use. Commercial inquiries or rights and permissions requests should be directed to the individual publisher as copyright holder.

# Lung Cancer Risk in Mice: Analysis of Fractionation Effects and Neutron RBE with a Biologically Motivated Model

W. F. Heidenreich,<sup>a,1</sup> B. A. Carnes<sup>b</sup> and H. G. Paretzke<sup>a</sup>

<sup>a</sup> GSF—Institute for Radiation Protection, 85764 Neuherberg, Germany; and <sup>b</sup> Reynolds Department of Geriatrics, University of Oklahoma College of Medicine, Oklahoma City, Oklahoma 73104

---

Heidenreich, W. F., Carnes, B. A. and Paretzke, H. G. Lung Cancer Risk in Mice: Analysis of Fractionation Effects and Neutron RBE with a Biologically Motivated Model. *Radiat. Res.* 166, 794–801 (2006).

Data from Argonne National Laboratory on lung cancer in 15,975 mice with acute and fractionated exposures to  $\gamma$  rays and neutrons are analyzed with a biologically motivated model with two rate-limiting steps and clonal expansion. Fractionation effects and effects of radiation quality can be explained well by the estimated kinetic parameters. Both an initiating and a promoting action of neutrons and  $\gamma$  rays are suggested. While for  $\gamma$  rays the initiating event is described well with a linear dose-rate dependence, for neutrons a nonlinear term is needed, with less effectiveness at higher dose rates. For the initiating event, the neutron RBE compared to  $\gamma$  rays is about 10 when the dose rate during each fraction is low. For higher dose rates this RBE decreases strongly. The estimated lifetime relative risk for radiation-induced lung cancers from 1 Gy of acute  $\gamma$ -ray exposure at an age of 110 days is 1.27 for male mice and 1.53 for female mice. For doses less than 1 Gy, the effectiveness of fractionated exposure to  $\gamma$  rays compared to acute exposure is between 0.4 and 0.7 in both sexes. For lifetime relative risk, the RBE from acute neutrons at low doses is estimated at about 10 relative to acute  $\gamma$ -ray exposure. It decreases strongly with dose. For fractionated neutrons, it is lower, down to about 4 for male mice. © 2006 by Radiation Research Society

---

## INTRODUCTION

During the period from 1971 to 1986, the JANUS Program in the Biological and Medical Research Division at Argonne National Laboratory (ANL) compiled a database of studies conducted to examine the response of both sexes of the F<sub>1</sub> hybrid mouse B6CF<sub>1</sub> (C57BL/6 × BALB/c) to external whole-body irradiation by <sup>60</sup>Co  $\gamma$  rays and by fission neutrons. These unique data allow the estimation of fractionation effects and of neutron RBE under various exposure patterns terminated at suitable times for many end points of interest in radiation risk estimation. The ANL data

have already been used to study radiation-induced risk for life shortening (1, 2), cancer (3) and other diseases (4).

Effects of fractionation, protraction and radiation RBE for neutrons have not yet been adequately derived for humans. For example, the single brief exposures of the atomic bomb survivors to  $\gamma$  rays cannot be used to test for protraction effects. In addition, the small neutron doses in those data make it impossible to estimate the contribution of neutrons with confidence (5). In general, the quality of dosimetry in the data for the larger human cohorts is inferior to that achieved in controlled animal experiments. Specifically, the extensively documented quality of the JANUS data makes this database an ideal choice for a quantitative examination of the effects of fractionation and of radiation quality on cancer induction processes.

Data of good quality for duration-of-life studies involving laboratory animals receiving whole-body external exposure to radiation are limited because of the great expense of these labor-intensive and time-consuming studies. These factors, as well as ethical considerations regarding animal experiments, suggest that existing databases like the one for the JANUS studies should be revisited periodically for advanced ways of analysis. New methods of analysis may reveal new information or reduce the uncertainty of radiobiologically relevant parameters that have been estimated previously.

Biologically motivated models for radiation-induced cancers are a case in point. These models aim to combine information from epidemiology, animal experiments and radiobiology to generate risk functions whose parameters have a biological meaning (e.g., mutation rates or clonal expansion rates) which in turn could be tested separately. In this paper, the well-studied two-step clonal expansion (TSCE) model (6, 7) will be applied to the JANUS data for the first time. It has already been used successfully e.g. to describe the protraction effects due to radon exposure in humans and rats (8, 9) and radium in mice (10). In contrast to earlier analyses of animal experiments, the exposure pattern is followed precisely here, without averaging over the period from the start of exposure to the first fraction to the end of the last fraction.

The parameters of biologically motivated models have

<sup>1</sup> Address for correspondence: GSF—Institute for Radiation Protection, 85764 Neuherberg, Germany; e-mail heidenreich@gsf.de.

inherent biological meaning. As such, they should be applied to pathological events arising from a common underlying mechanism to make conceptual sense. However, pathological specificity often conflicts with the sampling requirements needed for reliable statistical estimation. Lung cancer (here, alveogenic adenocarcinoma) will be the focus of this study because it is the most frequent carcinoma observed within the JANUS database.

Historically, analyses of the JANUS data have revealed (3) that protraction (fractions over a longer period) appears to enhance the effect of exposure to neutrons and diminishes the effect for exposure to  $\gamma$  rays. These protraction effects have yielded neutron RBE values for relative risk that range from about 5 to 25 depending on the fractionation pattern of exposure. The major motivation for the present work was to determine different radiation effects on the model parameters of a TSCE model and to explain this behavior.

## MATERIALS AND METHODS

### The Data Set

A data set for 15,975 mice from 112 experimental animal groups for which pathology information is available was used in this study. Except for a different selection of controls, these are the same data as described in ref. (3).

Three basic patterns of exposure for both radiation qualities and both sexes were applied: (a) single exposures of about 20 min, (b) 24-week-long once-weekly exposures, and (c) 60-week-long once-weekly exposures of typically 45 min each. Smaller groups of mice were also exposed to other patterns (e.g., 22 h per day, three or five times per week, for 24 or 60 weeks). The exposure patterns are described in detail in ref. (11). Some of the information is repeated here in Table 1. Exposure started at an age of about 110 days. All exposure patterns are used here exactly as given in this table. The dose rates are piecewise constant, in many groups with long zeros between short fractions. The dose rate during exposure is calculated from the number of fractions, their duration and the cumulative dose.

The groups belong to one of six different experimental series. The JM7 series has only males and the JM9 series has only female animals. The JM7 series has only exposed animals; all the other experimental groups have a matched control.

In a biologically motivated model, the particular cancer end point examined should be defined as narrowly as possible to keep the number of pathways to this end point as small as possible. The Argonne pathology database is made up of pathology codes organized into combined pathology end points. The end points considered for this analysis came from the histopathology database designated H (11). In total there are 5341 animals with carcinomas, of which 3918, i.e. more than half of all animals with carcinoma, have a lung cancer (alveogenic adenocarcinoma). Therefore, this end point was selected for analysis. A veterinary pathologist reviewed every pathology and made a judgment as to whether it caused death, contributed to death, or was simply incidental. The available data set uses lung tumors that either caused or contributed to death. Lung cancers that were classified as incidental were not included because they were only found by chance when the animal died of a different cause.

### The TSCE Model

The TSCE model has a long history; short introductions and references can be found in refs. (7, 12). More mathematical detail is provided in refs. (6, 13). Intermediate cells are created with the initiation rate  $\nu$  from

the pool of normal cells. These intermediate cells can divide into two intermediate cells with rate  $\alpha$  and die or differentiate with rate  $\beta$ . The net effect of these two processes is called promotion. The intermediate cells can also divide into an intermediate cell and a malignant cell with the transformation rate  $\mu$ .<sup>2</sup> The progression from a malignant cell to an observable tumor is characterized here only with a lag time  $t_{lag}$ . It is possible biologically that radiation could also act on progression, i.e. modify the lag time. Unfortunately, not all of these parameters can be determined from data (13). Therefore, only so-called identifiable parameters are used here. In principle, radiation action is possible on initiation, promotion and transformation. It is known that the respective contributions of these actions to the end point of interest can be separated by fitting the model to statistically sufficiently powerful data (14).

For the effect on the transformation rate as used in the model, it is well known that a sudden increase (e.g. by radiation action) in the transformation rate by a factor at a certain age leads to a jump with the same factor in the hazard rate for the first malignant cell. After an assumed fixed lag time  $t_{lag}$ , the same jump then occurs in the hazard for cancer at an age shifted by the lag time. For an acute exposure, a hazard with a short spike is the result in this model. This is highly unlikely, because the time from a single malignant cell to a fatal lung cancer is surely not a fixed time. Thus the approximation of a fixed lag time cannot be used in that case, but rather it has to be smeared out in time when a transforming action of an exposure is expected, as was done e.g. when modeling smoking (15). Reversing the reasoning, a transforming action of acute radiation exposures predicts a peak of cancer cases some time later. The shape of the peak is determined by the distribution of lag times. Inspection of the time dependence of the occurrence of early lung cancer cases among the present data set showed no evidence for this to happen. Therefore, an effect of radiation on transformation plays no significant role in the present situation. The technical complications of accounting for a transforming action of radiation were left out, but tests were performed to determine whether the model and parameters obtained do indeed also correctly describe the early cases among the acutely exposed animals.

Initiation and promotion at a given time is assumed to be dependent on dose rate at that time. The animals in the data set either are controls or are exposed to  $\gamma$  rays or to neutrons, but no animals are exposed to both radiation types. Therefore, in the formulas below, the dose rate  $d$  is  $d_\gamma$  for data for  $\gamma$  rays or  $d_n$  when data for neutron exposure are analyzed. The parameters in the formulas below have a subscript. When the type of exposure is also indicated in a parameter, a superscript  $\gamma$  or  $n$  is added.

The dose rates are derived from the data in Table 1. For example, the two groups GBI and GEI have the same dose of 8.2 Gy with 24 fractions of (calculated) 342 mGy each. For group GBI each fraction is delivered in 45 min, giving a dose rate of 7.6 mGy/min, while in group GEI it is delivered in 360 min, giving a dose rate of 0.95 mGy/min during the exposure. Averaging over the period from first exposure to last exposure would give the same dose rate in the two groups.

The quotient of the initiation rate with dose rate  $d$  over the spontaneous initiation rate is assumed to be of the form

$$\frac{\nu(d)}{\nu(0)} = 1 + \nu_{lin} d e^{-\nu_{exp} d}. \quad (1)$$

The parameter  $\nu_{exp}$  allows to test for a nonlinear dependence of initiation on dose rate.

The effective clonal expansion rate  $\gamma(d) \equiv \alpha(d) - \beta(d) - \mu(d)$  is allowed to be dependent on the dose rates such that it is linear with coefficients  $\gamma_{lin}$  at low rates and levels to a value of  $\gamma_0 + \gamma_{level}$  at high dose rates, as in earlier work on high-LET radiation (9),

$$\gamma(d) = \gamma_0 + \gamma_{level} [1 - e^{-(\nu_{lin} d / \gamma_{level})}]. \quad (2)$$

The parameters in these equations are estimated, in addition to those

<sup>2</sup> The term transformation is used here for the rate-limiting transition event from an intermediate cell to a malignant one, not for the whole process from a healthy to a malignant cell.

TABLE 1  
Some Properties of the Groups

JM series	Group	Duration (weeks) × fractions	Cumulative dose (Gy)	Duration of fraction (min)	Male				Female			
					Animal	Observed	Exposed	Spontaneous	Animal	Observed	Exposed	Spontaneous
13	C0X	0	0.0		196	33	33.0	33.0	214	20	16.8	16.8
2	CAC	0	0.0		123	60	58.9	58.9	124	24	26.5	26.5
2	CEC	0	0.0		137	71	71.2	71.2	165	32	29.1	29.1
4	CK0	0	0.0		129	52	42.8	42.8	110	14	14.0	14.0
4	CL0	0	0.0		111	26	28.9	28.9				
4	CLC	0	0.0		120	28	21.4	21.4				
2	CS0	0	0.0		174	75	79.1	79.1	185	29	36.3	36.3
3	CS0	0	0.0		142	43	41.7	41.7	152	17	17.9	17.9
9	CXC	0	0.0						248	31	27.1	27.1
9	GX1	1 × 1	0.26	20					177	18	19.4	17.6
9	GX2	1 × 1	0.43	20					121	16	17.5	14.5
9	GX3	1 × 1	0.86	20					73	8	9.1	6.4
2	GS1	1 × 1	0.86	20	328	153	157.2	126.3	367	77	67.8	46.6
3	GS4	1 × 1	0.86	20	138	45	46.0	37.1	171	23	26.4	18.4
3	GS5	1 × 1	1.4	20	113	43	39.7	28.7				
3	GS6	1 × 1	2.0	20	122	36	37.1	23.6				
2	GS2	1 × 1	2.6	20	155	73	58.2	32.9	183	37	29.7	12.1
3	GS7	1 × 1	4.0	20	102	31	29.4	13.4	49	18	9.1	2.7
3	GS8	1 × 1	5.5	20	99	16	20.2	7.5	66	4	8.6	2.0
2	GS3	1 × 1	7.6	20	133	19	24.7	7.3	136	9	11.1	1.8
4	GK1	24 × 1	2.0	45	391	119	125.2	87.9				
4	GK2	24 × 1	4.0	45	278	110	94.6	49.3	329	53	53.0	19.5
2	GBI	24 × 1	8.2	45	132	63	70.3	21.9	112	33	33.0	5.9
2	GEI	24 × 1	8.2	360	113	66	61.5	19.0	105	26	31.5	5.6
4	GK3	24 × 1	9.2	45	146	41	42.3	11.5				
2	GDI	24 × 1	10.6	45	115	56	49.7	12.0	166	43	40.2	5.0
4	GK4	24 × 1	18.4	20	105	17	9.4	1.0				
4	GL1	24 × 5	2.1	1320	118	27	35.3	25.2				
4	GL2	24 × 5	4.2	1320	57	16	21.0	11.4				
2	GAI	24 × 3	8.2	15	113	59	64.4	20.1	78	22	26.9	5.0
4	GL3	24 × 5	9.6	1320	48	10	12.8	3.5				
4	GL4	24 × 5	19.2	1320	30	4	6.8	0.8				
13	G1X	60 × 1	1.0	20	212	43	36.9	32.4	223	18	21.8	17.7
13	G2X	60 × 1	1.9	20	115	18	21.8	16.9	127	10	12.0	8.1
13	G3X	60 × 1	3.0	20	57	8	9.1	6.3	59	9	4.1	2.3
7	GQ1	60 × 1	4.1	45	92	28	34.6	21.3				
13	G4X	60 × 1	4.5	20	62	11	11.2	6.6	57	6	5.9	2.6
13	G5X	60 × 1	6.0	20	56	8	9.1	4.6	59	4	6.3	2.2
7	GQ2	60 × 1	19.0	45	124	41	34.4	5.8				
4	GL5	60 × 5	5.3	20	121	27	30.4	16.9				
4	GL6	60 × 5	10.7	20	79	16	20.2	6.7				
4	GL7	60 × 5	24.6	20	51	18	20.1	2.3				
9	NX4	1 × 1	0.01	20					253	22	26.5	25.0
9	NX5	1 × 1	0.02	20					169	11	15.8	13.8
9	NX6	1 × 1	0.05	20					132	12	13.2	10.3
9	NX7	1 × 1	0.09	20					91	6	10.0	6.5
9	NX8	1 × 1	0.19	20					78	12	8.8	4.3
2	NS1	1 × 1	0.19	20	335	144	154.0	113.1	343	64	69.3	33.3
3	NS4	1 × 1	0.19	20	189	59	62.5	46.0	208	37	36.5	17.6
3	NS5	1 × 1	0.38	20	153	50	54.0	33.9				
9	NX9	1 × 1	0.38	20					123	15	13.6	4.8
3	NS6	1 × 1	0.57	20	169	64	57.4	33.2				
2	NS2	1 × 1	0.75	20	157	67	62.1	34.3	173	30	36.5	9.7
3	NS7	1 × 1	1.13	20	104	30	25.0	13.7				
3	NS8	1 × 1	1.5	20	101	19	22.5	12.9	99	14	13.4	3.3
2	NS3	1 × 1	2.3	20	135	21	24.3	16.0	167	17	15.4	4.4
4	NK1	24 × 1	0.19	45	328	118	109.9	82.3	496	66	70.2	36.8
4	NK2	24 × 1	0.38	45	259	93	86.2	51.1				
4	NK3	24 × 1	0.57	45	139	39	46.1	22.4				
2	NDI	24 × 1	0.75	45	115	57	43.8	18.3	147	54	40.8	7.6

**TABLE 1**  
**Continued**

JM series	Group	Duration (weeks) × fractions	Cumulative dose (Gy)	Duration of fraction (min)	Male				Female			
					Animal	Observed	Exposed	Spontaneous	Animal	Observed	Exposed	Spontaneous
4	NK4	24 × 1	1.1	45	121	35	37.1	11.3				
4	NK5	24 × 1	1.6	45	110	33	34.6	7.9	127	32	27.6	1.9
2	NBI	24 × 1	2.26	45	101	36	30.9	5.2	97	27	24.6	1.0
2	NEI	24 × 1	2.26	360	119	51	55.6	8.0	100	25	30.7	1.0
2	NAI	24 × 3	2.26	15	118	50	59.3	10.2	81	22	26.0	1.1
13	N1X	60 × 1	0.012	20	174	39	35.1	34.4	218	19	22.0	20.8
13	N2X	60 × 1	0.077	20	94	18	20.0	18.4	95	12	8.3	6.8
13	N3X	60 × 1	0.14	20	78	14	18.7	16.2	104	11	8.5	6.1
13	N4X	60 × 1	0.22	20	94	21	15.2	12.2	111	6	11.0	6.7
13	N5X	60 × 1	0.31	20	102	19	17.8	13.2	121	11	12.0	6.2
7	NQ1	60 × 1	0.38	45	95	42	41.2	28.4				
13	N6X	60 × 1	0.41	20	67	13	10.5	7.1	65	8	5.1	2.2
7	NQ2	60 × 1	1.5	45	127	42	42.9	13.8				

*Notes.* The expected numbers of cases and the expected spontaneous cases are based on the IP model; in the control groups, only the numbers for the  $\gamma$ -ray model are given.

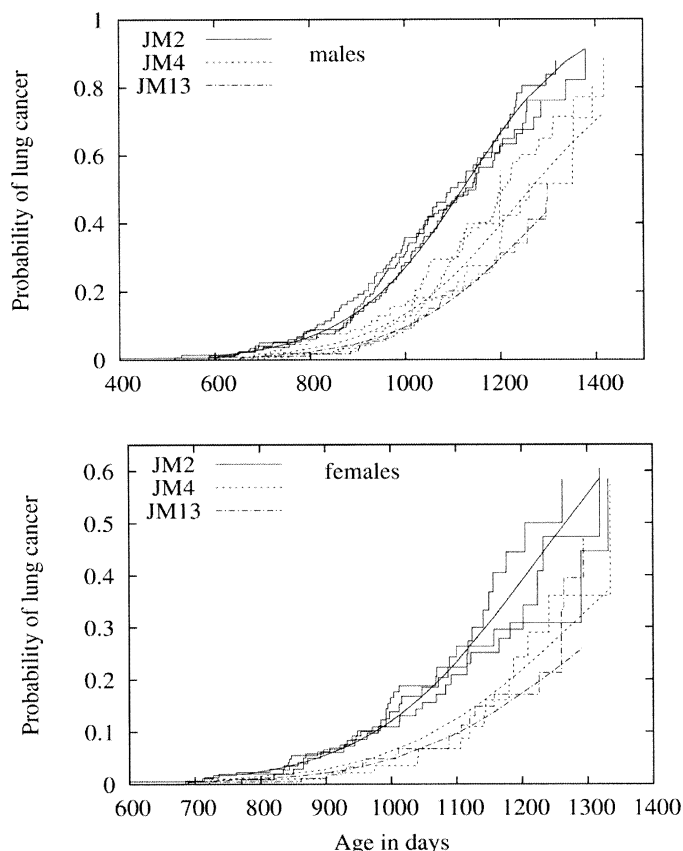


**FIG. 1.** Kaplan-Meier plots of the control groups in the data. The key distinguishes between the various experimental series, some of which contain several control groups. Data on the series JM3 and JM9 are left out to avoid clutter. They lie in between. The female mice have a much lower lung cancer risk than the males. Therefore, different scales are used for the two sexes. The smooth lines are the probability of lung cancer from the IP model fitted to the controls and the animals exposed to  $\gamma$  rays.

that affect the background only: the product  $Y_0 \equiv \nu(0)\mu(0)$  of the spontaneous initiation and transformation rates, and the stochasticity parameter  $q$ , which can give a leveling of hazard to  $Y(0)/q$  at high age. The model as formulated allows calculation of the hazard for the first malignant cell. To allow for a finite time to the observable lung cancer, a lag time  $t_{lag}$  is introduced, which also must be estimated from the data.

There are complications that can be seen in the Kaplan-Meier plots for lung cancer probabilities of control groups in Fig. 1. Female mice have a much lower lung cancer risk. This confirms the notion that the two sexes must be kept apart in the modeling, and two lung cancer models, one for males and one for females, are estimated. Within one sex, the differences between the control groups of different experimental series are substantial, while those within a series agree reasonably. This may point to a varying risk of lung cancer in the animals used at the different experimental series, possibly due to genetic, epigenetic, environmental or other factors that are not quantified. To correct for them, an experiments factor is introduced: The hazard is made dependent on the experimental series. For each of the two sexes, five numbers  $f(\text{experimental series})$  are estimated, which are additional multiplicative factors in the hazard. Each of them affects only the respective experimental series. To prevent non-identifiability,  $Y_0$  is fixed to an arbitrary number. Such overall factors to the hazard function were used earlier to take birth year effects in human cohorts into account (8, 16). To our knowledge such factors have not been used in earlier analyses of these data. The different rates among the controls have been taken into account by comparing exposed animals only with their own controls (4).

For each sex, two parameter sets are estimated, one for  $\gamma$  rays and one for neutrons. In principle, it would be possible to use the same background parameters in both cases, but tests showed that a better fit of the exposed groups can be obtained with this procedure.

*Likelihoods and Quality of Fit*

The mathematical formulation of the TSCE model allows one to calculate the hazard  $h$  and the respective “survival” probability  $S$  (probability that no lung cancer occurred) at the age of death. These functions depend on age, sex, experimental series, and exposure history of the animal as well as on the identifiable parameters given above. The recursive formulas from ref. (13) are used to calculate them. A time at risk from the beginning of follow-up is used. Model fitting is done by maximizing the log-likelihood

$$\ln L = \sum_{\text{nocancer}} \ln S + \sum_{\text{cancer}} \ln(hS), \tag{2}$$

**TABLE 2**  
**Comparison of Various Models Showing the**  
**Number of Fitted Parameters**

Model	Deviance		Number of parameters
	Male	Female	
<b><math>\gamma</math> rays</b>			
IP model	24,104.2	9677.8	12
With $\nu_{\text{exp}}^{\gamma}$	-0.9	-0.0	13
No P	+31.5	+9.2	10
No I	+61.8	+38.3	11
No dose dependence	+337.4	+200.1	8
<b>Neutrons</b>			
IP model	23,803.8	11,531.0	13
No P	+3.8	+26.7	11
No I	+14.1	+96.7	11
No dose dependence	+301.5	+401.8	8

*Notes.* For the IP model, the deviance is given. For the other models, the difference in deviance relative to the IP model are shown. Lower values indicate a better fit to the data. I denotes initiation, P promotion.

where the sum are over all animals with and without lung cancer. The dependences of  $h$  and  $S$  on the animal number, and the quantities given above are omitted, to keep the formula simple. This form assumes that lung cancers in the mice are fatal. The deviance is

$$\text{Dev} = -2 \ln L_{\text{max}} \quad (4)$$

for the maximum likelihood. Parameter uncertainties are calculated using the profile likelihood technique and the Fisher information matrix of second derivatives. These estimations were done with the function minimizer MINUIT from CERN (17).

As a means for judging the quality of fits, for each group the number of expected cases is calculated by summing over all animals the cumulative hazard of each animal during the follow-up. Also, the Kaplan-Meier estimate of the probability of tumor is calculated and compared with the one from the fitted model, separately for each experimental group.

The fitted model predicts the hazard function of lung cancer for arbitrary exposures to  $\gamma$  rays and neutrons in the hybrid mice. It allows one to calculate derived quantities like e.g. lifetime relative risk (LRR) for a fixed average survival time, neutron RBE for risk, etc. in a straightforward way. Those that are presented here are chosen such that interesting effects in the data set—like fractionation effects—are highlighted.

The fitted model includes estimates for the dose-rate dependence of the various kinetic parameters of the TSCE model.

## RESULTS

The deviances of some of the model fits are given in Table 2 separately for the two sexes and the two radiation qualities. Also given is the number of estimated parameters. The IP model (initiation and promotion) is the preferred model in both cases. It has the parameters described above, except that there is no nonlinearity in initiation for  $\gamma$  rays. The other fitted models are described relative to this one. Including the nonlinearity  $\nu_{\text{exp}}^{\gamma}$  for  $\gamma$  rays gives an improvement in the case of male mice, but not a significant one. Contrary to this, for neutrons it does provide a significant improvement (not shown). Leaving out a promoting action of radiation gives an increase of deviance, which is significant except for neutron exposure in the data sets for male mice. A stronger increase in deviance is found when no initiating action of radiation is assumed. An action of radiation on both initiation and promotion is favored by the data. But each of these two radiation actions alone can already describe a large part of the radiation effect, compared to the numbers when no radiation effect is included. Fixing the series factors to 1 and estimating  $Y_0$  instead gives a dramatic decrease in the quality of fit (not shown).

The estimated parameter values of the IP model and their confidence bounds are listed in Table 3. The confidence bounds are calculated with lag time fixed to stabilize the calculations (see below). They are significantly different from 0, except for the estimations for a promoting action of neutrons in the male mice. Each of the four models has eight estimated parameters for describing the spontaneous background. The models for  $\gamma$  rays have three more parameters, the ones for neutrons four more parameters. With this large number of parameters it is mandatory to make sure that they can be estimated reliably from the data. They were chosen such that from earlier experience with other data sets it could be expected that they can be determined from this data set. The given confidence intervals are a simple test to confirm this.

At low dose rates, the parameters of the linear part of the radiation actions are most important. A suitable way to

**TABLE 3**  
**Maximum Likelihood Estimates (MLE) for the Dose-Response Parameters of the IP**  
**Models and their Confidence Bounds**

Parameter	Male		Female	
	MLE	CI (95%)	MLE	CI (95%)
<b><math>\gamma</math> rays</b>				
$\nu_{\text{lin}}^{\gamma}$ [(mGy/day) <sup>-1</sup> ]	0.076	(0.052, 0.010)	0.14	(0.071, 0.24)
$\gamma_{\text{lin}}^{\gamma}$ [(10 <sup>4</sup> mGy) <sup>-1</sup> ]	0.75	(0.49, 1.01)	1.2	(0.37, 2.0)
$\gamma_{\text{level}}^{\gamma}$ [day <sup>-1</sup> ]	22	(3, inf)	60	(1, inf)
<b>Neutrons</b>				
$\nu_{\text{lin}}^{\text{n}}$ [(mGy/day) <sup>-1</sup> ]	0.72	(0.29, 1.13)	1.90	(1.20, 2.82)
$\nu_{\text{exp}}^{\text{n}}$ [(10 <sup>4</sup> mGy/day) <sup>-1</sup> ]	0.14	(0.05, 0.21)	0.11	(0.07, 0.17)
$\gamma_{\text{lin}}^{\text{n}}$ [(10 <sup>4</sup> mGy) <sup>-1</sup> ]	3.7	(0, 12)	8.1	(5.0, 11)
$\gamma_{\text{level}}^{\text{n}}$ [day <sup>-1</sup> ]	1.6	(0, inf)	8.2	(1.9, 15)

**TABLE 4**  
**Doubling Dose Rates and Their Neutron RBE**  
**Calculated from the Linear Part of Initiation**

	Male	Female
$\gamma$ rays (mGy/day)	13	7.1
Neutrons (mGy/day)	1.4	0.53
RBE	9.2	13

look at the initiating action at low dose rates is to calculate the dose rate  $1/\nu_{lin}$ , which doubles the spontaneous values, when the linear term only is considered. These dose rates are given in Table 4.

The estimated parameter values of the IP model for the background cancer risk depend on the control animals and the exposed ones. The estimated factors for the experimental series differ by a factor of up to 3.1 for males and 2.4 for females, with JM2 highest and JM13 lowest. This applies to both sexes in a strikingly similar way. The estimated lag time is about 250 days in the models for the  $\gamma$  rays and about 170 days in the models for neutrons. It has been verified that the uncertainties of this lag time are large by fixing it to selected values. The standard tools of MINUIT cannot be used for this purpose, because the ages are given discretely, in days. Therefore, the deviances depend on the lag time in a way that is too coarse to draw conclusions from the matrix of second derivatives (Fisher information matrix), and the profile-likelihood calculation also becomes unreliable. The true lag time of the controls cannot depend on the radiation quality. But the lag time can best be estimated from time since exposure, so the statistical power is coming mostly from the groups with high dose.

For the IP models, the expected number of cases for the various experimental groups is given in Table 1 along with the number expected from the model for spontaneously occurring lung tumors. For the correct model, the observed cases are Poisson-distributed around the expected cases. This allows calculation of the standard errors for each group. The sum of the standard errors in all 112 groups is 86.7: The observed numbers of cases in the groups are described well by the IP model. In Fig. 2, the Kaplan-Meier estimates of the probability of tumor incidence and the ones expected from the IP model are plotted for some of the groups. This shows that the observed age dependences are also reproduced well.

The resulting relative risk functions are plotted in Fig. 3 for some of the groups. The risks for neutrons arise earlier due to the shorter estimated lag time. The time-since-exposure dependence of the relative risk is quite strong. Therefore, the relative risk at a fixed age is not a good quantification of risk. The lifetime relative risk (LRR) is a better quantity. In Fig. 4 it is plotted at a mean lifetime of 900 days for exposures with fractionation patterns as in the data set. For  $\gamma$  rays there is a weak fractionation effect (more fractions over a longer period give less effect). For neutrons at low doses, the same pattern is found, while at

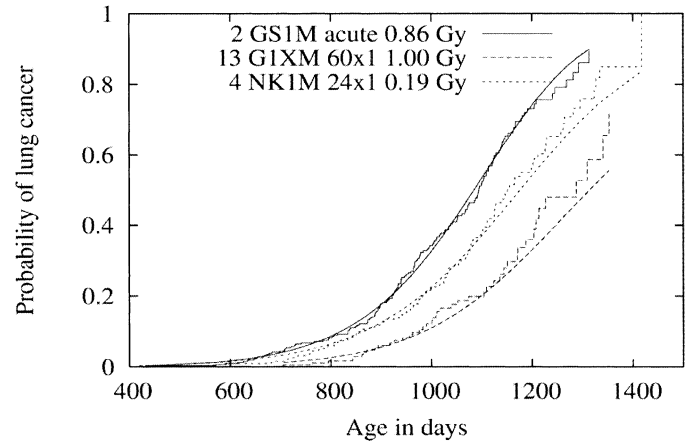


**FIG. 2.** Kaplan-Meier plots and prediction of the IP model for the probability of lung cancer for a few classes. They are selected for having a large number of animals and cases. Note that they belong to different experimental series and thus have different background rates. The key gives the experimental series, the group, the sex, the duration and the dose.

doses above about 0.3 Gy the acute exposure has a lower effect than the fractionated ones. Note that all exposures used in this figure start at 110 days, so that the same total dose is delivered at different ages for the different fractionation schemes. The nonlinear form of LRR for the acute neutrons comes from the nonlinearity term  $\nu_{exp}''$ . Females have larger relative risks than males.

The estimated radiation RBE for LRR relative to acute  $\gamma$  rays at an age of 110 days is plotted in Fig. 5. As was observed before (3), it is strongly dependent on the exposure duration and the exposure rate. (Note that the RBE values in that table are comparing neutrons and  $\gamma$  rays of the same exposure pattern.)

**DISCUSSION**

The biologically motivated TSCE model can describe the occurrence of the end point lung cancer in this complicated

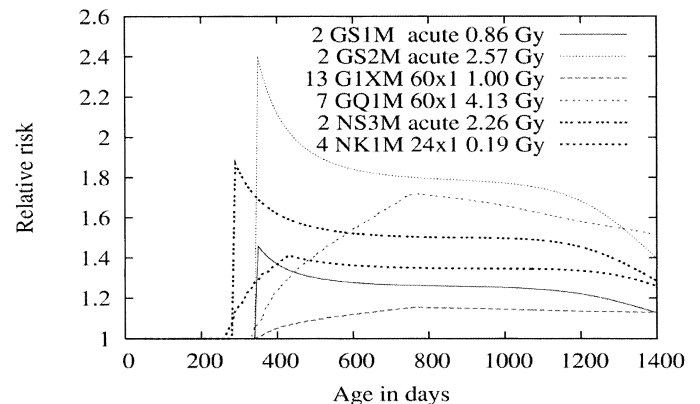


**FIG. 3.** Estimated relative risk functions for some of the exposed groups. The start of exposure differs by a few days between the groups. The exposure duration helps to separate between the lines. The key gives the experimental series, the group, the sex, the duration and the dose.

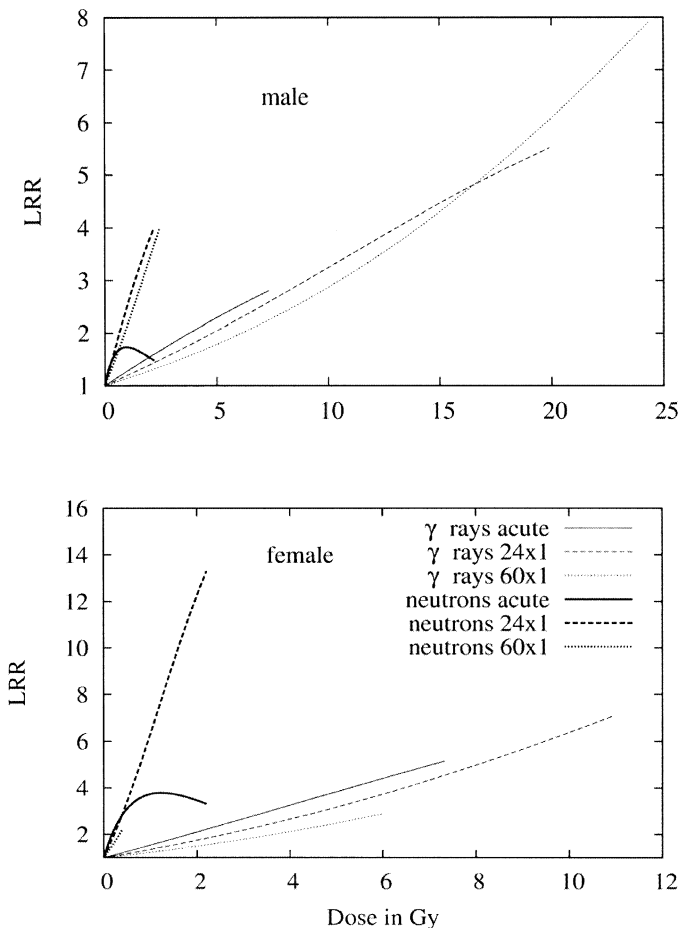


**FIG. 4.** Estimated lifetime relative risk at an age of 900 days for exposures with fractionation patterns as in the data. The lines are cut off at the highest dose with the exposure patterns in the data set.

data set well. The main features of the data, like fractionation effects and effects of radiation quality, can be explained within the model by statements about the kinetic parameters.

#### Comparison with Human Risks

The LRR at 1 Gy of acute  $\gamma$  rays at 110 days is 1.27 for males and 1.53 for female mice. These numbers can be compared with the site- and sex-specific risk estimates from the atomic bomb survivors, adjusted to age at exposure 30 (18), which are 1.33 for males and 1.75 for females; see also (19, 20). For doses less than 1 Gy, the RBE for LRR of exposure to  $\gamma$  rays in several fractions compared to one fraction is between 0.4 and 0.7 in both sexes (Fig. 5). So the LRR from the more protracted exposure under 1 Gy is about half of the acute exposure. This agrees well with a DDREF of about 2. But note that the animals were exposed from about the same age, so that more protracted exposure is in part given at a later age. An exposure later in life tends to give less effect. Further research is needed to better understand the mechanisms that may lead to a DDREF different from 1 (21).

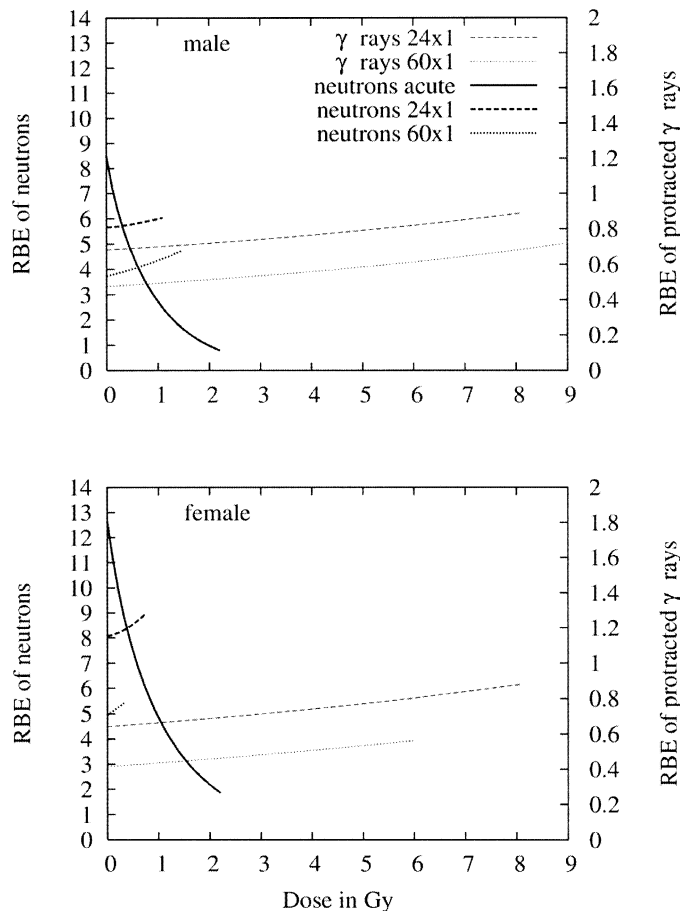


**FIG. 5.** RBE for the end point LRR relative to acute (1 week)  $\gamma$ -ray exposure at 110 days of age.

#### Neutron RBE

The neutron RBE for LRR of acute neutrons at the low doses is estimated at about 10 relative to the acute  $\gamma$  rays. It is strongly decreasing with dose. As was stressed above, the decrease depends on the nonlinear dependence of initiation on neutron dose rate, which is induced from data at higher doses. For fractionated neutrons, the RBE is substantially lower, down to about 4 in the male mice. The statistical power of the present data set at neutron doses below 0.2 Gy is not large. Results using mice exposed to neutrons at such doses indicate that the dose response is linear (2). This could be accounted for in the present model by replacing the traditional dose-rate dependence in Eq. (1) by an expression in which a nonlinearity at high dose rates does not induce a nonlinearity at low dose rates.

The substantially lower effectiveness of acute neutrons at the higher dose range compared to the protracted exposure is mostly due to this nonlinear initiation.

#### Properties of the Fitted Model

These features of the risk functions are coming from the kinetic parameters of the TSCE model. Both an initiating and a promoting action of neutrons and  $\gamma$  rays are needed

to describe the observed data. A transforming action of the radiation should show most clearly in the acutely exposed animals. No signals are seen in this data set. These patterns are in good agreement with what was found on the radiation action of  $\alpha$  particles in lung (8) and in liver (2).

While for  $\gamma$  rays the initiating event is described well with a linear dose-rate dependence, for neutrons a nonlinear term is favored, with less effect per unit of dose at higher dose rates. The RBE for the initiating event in the low-dose-rate linear slope is about 10. It decreases strongly for higher dose rates.

The statistical approach used here uses all the available individual data. The fractionation patterns are in detail followed by the model. In this way, the application of the TSCE model here differs from earlier uses, where exposures were averaged over selected periods.

The different estimates of the lag time for  $\gamma$  rays and for neutrons may be interpreted as an indication that the time from a malignant cell to the death of the animal may be dependent on the radiation quality and/or the radiation dose. Such a situation could arise when different exposures cause e.g. genomic instability, which in turn might change the tumor growth rates. The present versions of the TSCE model cannot describe such a process.

#### ACKNOWLEDGMENTS

It is our pleasure to thank Dr. M. Fry for valuable comments on an earlier version of this paper. This work was supported by the EU under contract number FIGH-1999-00005 and FI6R-CT-2003-508842. The contributions made by BAC were supported by the National Aeronautics and Space Administration (NAG9-1518).

Received: November 11, 2005; accepted: May 18, 2006

#### REFERENCES

1. B. A. Carnes, D. Grahn and J. F. Thomson, Dose-response modeling of life shortening in a retrospective analysis of the combined data from the JANUS program at Argonne National Laboratory. *Radiat. Res.* **119**, 39–56 (1989).
2. B. A. Carnes and D. Grahn, Issues about neutron effects: The JANUS program. *Radiat. Res.* **128** (Suppl.), S141–S146 (1991).
3. D. Grahn, L. S. Lombard and B. A. Carnes, The comparative tumorigenic effects of fission neutrons and cobalt-60  $\gamma$  rays in the B6CF<sub>1</sub> mouse. *Radiat. Res.* **129**, 19–36 (1992).
4. B. A. Carnes, N. Gavrilova and D. Grahn, Pathology effects of radiation doses below those causing increased mortality. *Radiat. Res.* **158**, 187–194 (2002).
5. W. F. Heidenreich and H. G. Paretzke, City-effects in the atomic bomb survivors data atomic bomb survivors data. *Math. Comput. Model.* **33**, 1431–1438 (2001).
6. S. H. Moolgavkar and G. Luebeck, Two-event model for carcinogenesis: Biological, mathematical, and statistical considerations. *Risk Anal.* **10**, 323–341 (1990).
7. W. F. Heidenreich and H. G. Paretzke, Biologically based models of radiation-induced cancer. *Radiat. Res.* **156**, 678–681 (2001).
8. E. G. Luebeck, W. F. Heidenreich, W. D. Hazelton, H. G. Paretzke and S. H. Moolgavkar, Biologically based analysis of the Colorado uranium miners cohort data: Age, dose and dose-rate effects. *Radiat. Res.* **152**, 339–351 (1999).
9. W. F. Heidenreich, P. Jacob, H. G. Paretzke, F. T. Cross and G. E. Dagle, Two-step model for fatal and incidental lung tumor risk in rats exposed to radon. *Radiat. Res.* **151**, 209–217 (1999).
10. W. F. Heidenreich, W. A. Müller, H. G. Paretzke and M. Rosemann, A two-stage clonal expansion model for bone cancer risk in mice exposed to <sup>224</sup>Ra: Protraction effects from promotion. *Radiat. Environ. Biophys.* **44**, 61–67 (2005).
11. D. Grahn, B. J. Wright, B. A. Carnes, F. S. Williamson and C. Fox, *Studies of Acute and Chronic Radiation Injury at the Biological and Medical Research Division, Argonne National Laboratory, 1970–1992: The JANUS Program Survival and Pathology Data*. Technical Report ANL-95/3, Argonne National Laboratory, Argonne, IL, 1995.
12. S. H. Moolgavkar, Carcinogenesis models: An overview. In *Physical and Chemical Mechanisms in Molecular Radiation Biology* (W. A. Glass and M. N. Varma, Eds.), pp. 387–395. Plenum Press, New York, 1991.
13. W. F. Heidenreich, E. G. Luebeck and S. H. Moolgavkar, Some properties of the hazard function of the two-mutation clonal expansion model. *Risk Anal.* **17**, 391–399 (1997).
14. W. F. Heidenreich, Signals for a promoting action of radiation in cancer incidence data. *J. Radiol. Prot.* **22**, A71–A74 (2002).
15. W. F. Heidenreich, J. Wellmann, P. Jacob and H. E. Wichmann, Mechanistic modelling in large case-control studies of lung cancer risk from smoking. *Stat. Med.* **21**, 3055–3070 (2002).
16. W. F. Heidenreich, E. G. Luebeck, W. D. Hazelton, H. G. Paretzke and S. H. Moolgavkar, Multistage models and the incidence of cancer in the cohort of atomic bomb survivors. *Radiat. Res.* **158**, 607–614 (2002).
17. F. James, *MINUIT—Function Minimization and Error Analysis*, Version 94.1. CERN, Geneva, 1994.
18. D. A. Pierce, Y. Shimizu, D. L. Preston, M. Vaeth and K. Mabuchi, Studies of the mortality of atomic bomb survivors Report 12, Part I. Cancer: 1950–1990. *Radiat. Res.* **146**, 1–27 (1996).
19. D. L. Preston, Y. Shimizu, D. A. Pierce, S. Suyama and K. Mabuchi, Studies of mortality of atomic bomb survivors. Report 13: Solid cancer and noncancer disease mortality: 1950–1997. *Radiat. Res.* **160**, 381–407 (2003).
20. D. L. Preston, D. A. Pierce, Y. Shimizu, H. M. Cullings, S. Fujita, S. Funamoto and K. Kodama, Effects of recent changes in atomic bomb survivor dosimetry on cancer mortality risk estimates. *Radiat. Res.* **162**, 377–489 (2004).
21. National Research Council, Committee to Assess Health Risks from Exposure to Low Levels of Ionizing Radiation, *Health Risks from Exposure to Low Levels of Ionizing Radiation (BEIR VII, Phase 2)*. National Academies Press, Washington, DC, 2006.
22. J. B. Storer and R. J. M. Fry, On the shape of neutron dose-effect curves for radiogenic cancers and life shortening in mice. *Radiat. Environ. Biophys.* **34**, 21–27 (1995).
23. W. F. Heidenreich, U. Nyberg and P. Hall, A biologically based model for liver cancer risk in the Swedish Thorotrast patients. *Radiat. Res.* **159**, 656–662 (2003).